






OPEN ACCESS

Original research

Aspirin treatment prevents inflammation in experimental bifurcation aneurysms in New Zealand White rabbits

Stefan Wanderer ^{1,2}, Basil Erwin Grüter ^{1,2}, Fabio Strange,¹ Gwendoline Boillat,^{1,2} Sivani Sivanrupan,² Jeannine Rey,^{1,2} Michael von Gunten,³ Luca Remonda,⁴ Hans Rudolf Widmer,⁵ Daniela Casoni,⁶ Lukas Anderegg,^{1,2} Javier Fandino,^{1,2} Serge Marbacher ^{1,2}

► Prepublication history and additional material is published online only. To view please visit the journal online (<http://dx.doi.org/10.1136/neurintsurg-2020-017261>).

¹Neurosurgery, Kantonsspital Aarau AG, Aarau, Switzerland
²Department for BioMedical Research, University of Bern, Cerebrovascular Research Group, Bern, Switzerland
³Institute of Pathology Laenggasse, Ittigen, Switzerland
⁴Department of Radiology, Division of Neuroradiology, Kantonsspital Aarau AG, Aarau, Aargau, Switzerland
⁵Neurosurgery, Inselspital Universitätsspital Bern, Bern, Switzerland
⁶Faculty of Medicine, University of Bern, Experimental Surgery Facility, Bern, Switzerland

Correspondence to

Dr Stefan Wanderer, Neurosurgery, Kantonsspital Aarau AG, Aarau 5001, Switzerland; stefan_wanderer86@gmx.de

Received 29 December 2020
Revised 24 February 2021
Accepted 25 February 2021



© Author(s) (or their employer(s)) 2021. Re-use permitted under CC BY-NC. No commercial re-use. See rights and permissions. Published by BMJ.

To cite: Wanderer S, Grüter BE, Strange F, et al. *J NeuroIntervent Surg* Epub ahead of print: [please include Day Month Year]. doi:10.1136/neurintsurg-2020-017261

ABSTRACT

Background Aneurysm wall degeneration is linked to growth and rupture. To address the effect of aspirin (ASA) on aneurysm formation under various wall conditions, this issue was analyzed in a novel rabbit bifurcation model.

Methods Bifurcation aneurysms created in 45 New Zealand White rabbits were randomized to vital (n=15), decellularized (n=13), or elastase-degraded (n=17) wall groups; each group was assigned to a study arm with or without ASA. At follow-up 28 days later, aneurysms were evaluated for patency, growth, and wall inflammation at macroscopic and histological levels.

Results 36 rabbits survived to follow-up at the end of the trial. None of the aneurysms had ruptured. Patency was visualized in all aneurysms by intraoperative fluorescence angiography and confirmed in 33 (92%) of 36 aneurysms by MRI/MRA. Aneurysm size was significantly increased in the vital (without ASA) and elastase-degraded (with and without ASA) groups. Aneurysm thrombosis was considered complete in three (50%) of six decellularized aneurysms without ASA by MRI/MRA. Locoregional inflammation of the aneurysm complex was significantly reduced in histological analysis among all groups treated with ASA.

Conclusion ASA intake prevented inflammation of both the periaurysmal tissue and aneurysm wall, irrespective of initial wall condition. Although ASA prevented significant growth in aneurysms with vital walls, this preventive effect did not have an important role in elastase-degraded pouches. In possible translation to the clinical situation, ASA might exert a potential preventive effect during early phases of aneurysm formation in patients with healthy vessels but not in those with highly degenerative aneurysm walls.

INTRODUCTION

Aneurysmal subarachnoid hemorrhage due to rupture of an intracranial aneurysm remains one of the most devastating neurological diseases with a high associated mortality and morbidity.^{1,2} Chronic inflammatory processes of the vessel wall are known to have an important role in intracranial aneurysm wall pathobiology that leads to further growth and rupture.^{3,4} In this context, the role of aspirin (ASA) as a potential protectant against intracranial

aneurysm rupture by antagonizing the inflammatory microenvironment has been elucidated in previous animal studies, human case-control studies, and histological analyses of human aneurysm domes sampled from unruptured and ruptured intracranial aneurysms.³⁻⁵⁻⁸

For instance, continuous ASA intake for 12 weeks was shown to reduce macrophage-mediated aneurysm wall signal intensity in MRI of human unruptured intracranial aneurysms.⁹ Additionally, compared with unruptured aneurysms, upregulation of prostaglandin E2 synthase-1 (PGES-1) and cyclooxygenase-2 (COX-2) was observed in ruptured specimens.⁵ Compared with the control group, regular ASA intake 3 months before microsurgical clipping decreased vessel wall signal intensity on MRI, lowered PGES-1 and COX-2 concentrations, and decreased levels of macrophages in aneurysm tissues.¹⁰ In a study of patients taking ASA for 6 months or more, similar vessel wall results were noted using high-resolution 3 Tesla (T) MRI.¹¹ A 10-year retrospective review of patients with multiple intracranial aneurysms showed that ASA significantly decreased the aneurysm growth rate over time.¹²

Nonetheless, information is lacking about the effect of ASA intake on the natural course of bifurcation aneurysms with vital and already degraded wall conditions. Therefore, in this experimental bifurcation aneurysm rabbit model, we specifically analyzed inflammation and aneurysm growth over time in groups with varied wall characteristics.

MATERIALS AND METHODS

Study design

To analyze the effects of ASA on aneurysm formation under various wall conditions in a rabbit model, bifurcation aneurysms were created in 45 New Zealand White rabbits (figure 1). Animals were randomly allocated to one of three groups as vital (n=15), decellularized (n=13), or elastase-degraded (n=17) using a web-based randomization system (www.sealedenvelope.com). Each group was then assigned to a study arm with or without ASA (n=6).

Primary outcomes were defined as aneurysm patency and aneurysm growth 28 days after its

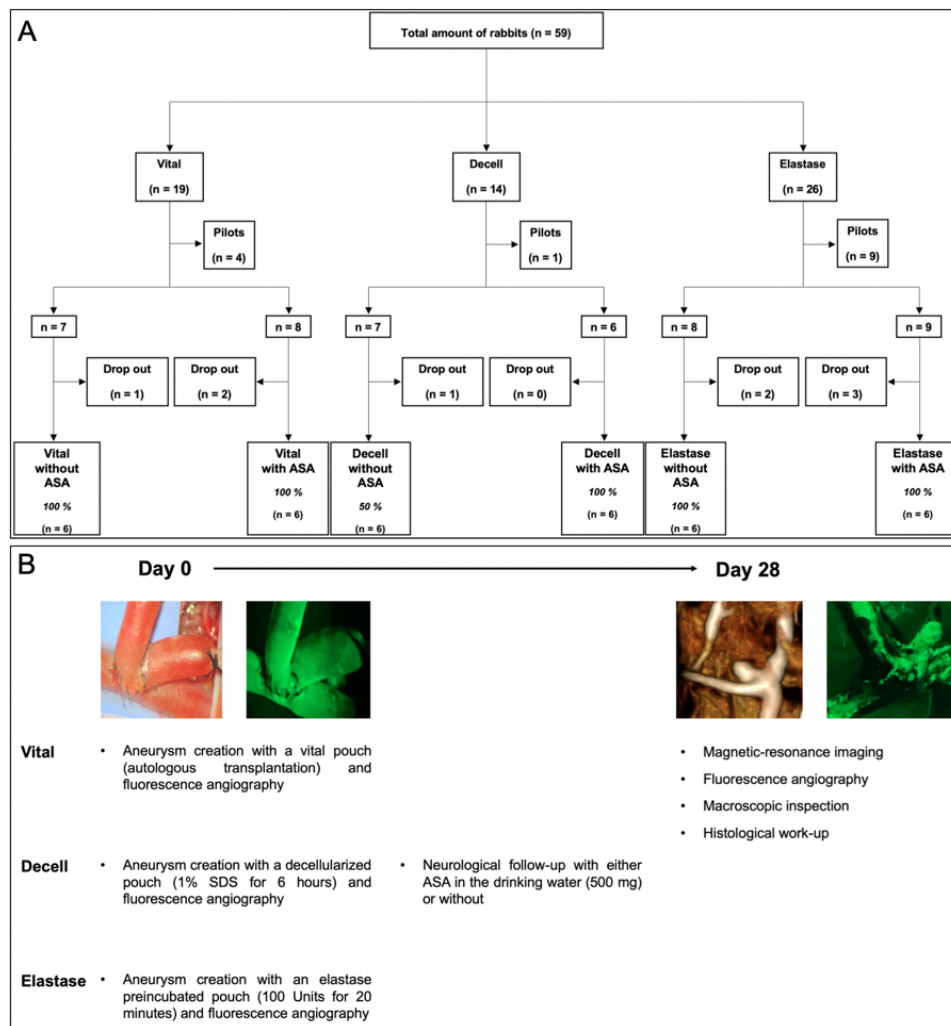


Figure 1 . Flowchart of the study design and follow-up modalities. Of 59 total animals, 36 were included for final analysis and 23 were excluded (ie, 14 in pilot study and 9 early dropouts (2 with complete thrombosis of the left parent artery; 3 with neurologic worsening; 1 with intraoperative digestion of the left carotid artery with subsequent euthanasia; 3 deaths of unknown causes) (Panel A). Patency of the aneurysm complex was confirmed via fluorescence angiography at day 0 intraoperatively, and with magnetic resonance angiography and fluorescence angiography 28 days after surgery (Panel B).

creation based on MRI findings. Secondary outcomes were aneurysm inflammation and thrombus organization. Patency of the aneurysm and its parent artery complex was controlled by fluorescence angiography at intraoperative creation and assessed at follow-up after terminal MRI.¹³ The study design is shown in figure 1.

Experiments were approved by the Local Committee for Animal Care of the Canton Bern, Switzerland (BE 108/16). The 45 female rabbits with a mean weight of 3722.64 g (± 276.34 g) and mean age of 16 weeks (± 3 days) were housed at room temperature of 22–24°C with a 12-hour light/dark cycle. The rabbits had free access to a pellet and hay diet as well as water. All animals received daily care in accordance with the local institutional guidelines. Animals allocated to the ASA groups exclusively had access to ASA water. Therefore, correct intake of ASA was calculated by monitoring drinking water twice daily. Surgeries were conducted in the Experimental Surgery Facility of the same department under supervision of a board-certified veterinary anesthesiologist. The ARRIVE guidelines were strictly followed.¹⁴

Bifurcation aneurysm model and surgical technique

Intraoperative surgical characteristics were recorded (see online supplemental figure 1). Detailed techniques of graft harvesting, graft preparation, and microsurgical creation of the arterial bifurcation have been described elsewhere.¹⁵ Briefly, bifurcation aneurysms were created by end-to-side anastomosis of the right common carotid artery (CCA) to the left CCA, and interposition of an arterial pouch in 36 female New Zealand White rabbits (see online supplemental figure 2 and online supplemental video 1).

Arterial wall degradation protocols

Considering the protocol without prior treatment, the autologous graft was harvested and directly transplanted to the same animal (autograft). Treatment followed either the sodium dodecyl sulfate (SDS) or the elastase protocol. For the SDS administration, tissue was decellularized according to a previously published protocol.⁴ For elastase administration, graft decellularization followed the details of a previously published protocol as well (detailed protocol in Supplementary Materials).¹⁵

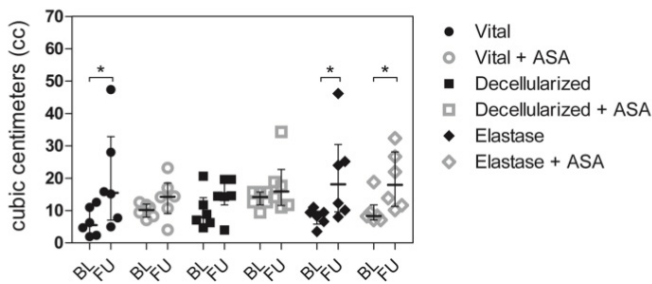


Figure 2 Bar graph comparing aneurysm volume (cc) at baseline (BL) and follow-up (FU). Vital aneurysms without ASA treatment showed significant patterns of growth whereas those with ASA treatment did not grow. All aneurysms with SDS-degenerated walls (with and without ASA treatment) did not grow. By contrast, all aneurysms that were degraded with elastase (without and with ASA treatment) showed significant growth during follow-up. All values are given as cubic centimeters (cc) and presented as median and interquartile range. * $p < 0.05$ vs. corresponding group.

Magnetic resonance imaging

Before final MRI, all animals were weighed and received a subcutaneous application of 0.1 mg/kg acepromazine (Prequillan, 10 mg/mL, Fatro, Italy) and buprenorphine (Temgesic, 0.3 mg/mL, Indivior AG, Switzerland) (0.03 mg/kg). Scanning time performed via 3 T Magnetom Skyra (Siemens, Munich, Germany) (see detailed protocol in Supplementary Materials) was 45 min per animal. On completion of fluorescence video angiography, the animals were euthanized by intravenous injection of 150–300 mg/kg pentobarbital (Esconarkon, 300 mg/mL, Streuli Pharma, Switzerland).

Measurement of the pre- and post-mortem aneurysm volumes

Aneurysms were measured and photographically documented before implantation. Aneurysm volume was calculated based on the formula: $\pi \times \text{height} \times \text{width}/2 \times \text{length}/2$. At final MRI, aneurysm volumes were quantified by 3D reconstruction (VitreaCore, Canon, Tokia, Japan); partial thrombogenesis was detected by this imaging and macroscopic evaluation (see online supplemental figure 3). Post-mortem macroscopical analysis and documentation of the aneurysm volume was carried out to assure a certain comparability.

Histology

For histological processing, paraffin-embedded aneurysms were cut in the axis of the underlying parent artery in 2 μm slices and stained, including hematoxylin-eosin (HE), smooth muscle actin (SMA), Masson-Goldner trichrome (MASA), and von Willibrand factor (F8). The slides were then digitized (Omnyx VL 120, GE, USA) and evaluated with a JVS viewer (JVS view 1.2 full version, <http://jvsmicroscope.uta.fi/software/>, Finland). The light microscopy findings were analyzed qualitatively by two observers (SW and SS) and rated with a previously used four-tier grading system.⁴ However, our study design precluded blinding of the three groups and the effect of ASA. Periadventitial inflammation, aneurysm wall inflammation, and neutrophils in the thrombus were evaluated in HE-stained slices, and periadventitial fibrosis was evaluated in MASA-stained slices. The presence of hematoma, cellularity, and dissection of the aneurysm wall and luminal thrombus were analyzed in HE-stained slices, whereas endothelium and neointima formation were evaluated in MASA-stained slices. Finally, aneurysm wall cellularity was

assessed in SMA-stained slices and endothelium in F8-stained slices.

Statistical analyses

All statistical analyses were calculated using the non-parametric Wilcoxon–Mann–Whitney U test and/or parametric unifactorial variance analysis. A p value of <0.05 and <0.01 was considered significant. Data were analyzed by IBM SPSS Version 22 (USA). The sample size per group was determined using an a priori sample size calculation (BiAS.for.Windows Version 11, Germany). To achieve $\alpha=0.05$ at $\beta=0.2$ with a sigma of 0.2, the sample size calculation showed that 4–8 animals per group were appropriate to achieve a delta between 0.3 and 0.5. Figures were visualized by Graph Pad Prism 8, Version 8.2.0.435 (GraphPad software, USA). All values are expressed as mean \pm SD or median (IQR).

RESULTS

Aneurysms in the vital group without ASA as well as in the elastase groups without and with ASA showed significant growth patterns over 28 days (figure 2). This effect was not observed in the vital group with ASA, nor in the decellularized groups without and with ASA.

Follow-up macroscopic measurements

Aneurysm size increased in all study groups from creation to follow-up (see online supplemental table 1). Specifically, aneurysm size increased in the vital group without ASA from $6.48 \pm 4.43 \text{ mm}^3$ at creation to $19.85 \pm 15.69 \text{ mm}^3$ at follow-up ($p < 0.05$) and with ASA from $10.01 \pm 2.13 \text{ mm}^3$ at creation to $13.91 \pm 6.38 \text{ mm}^3$ at follow-up ($p = 0.149$). Aneurysm size increased in the elastase group without ASA from $8.03 \pm 2.64 \text{ mm}^3$ at creation to $20.95 \pm 14.31 \text{ mm}^3$ at 28-day follow-up ($p < 0.05$) and with ASA from $9.91 \pm 4.48 \text{ mm}^3$ at creation to $19.46 \pm 8.99 \text{ mm}^3$ at follow-up ($p < 0.05$). Aneurysm size increased, although not significantly, in the decellularized group without ASA from $9.88 \pm 5.79 \text{ mm}^3$ at creation to $14.43 \pm 9.02 \text{ mm}^3$ at follow-up ($p = 0.261$) and with ASA from $13.61 \pm 2.56 \text{ mm}^3$ at creation to $17.96 \pm 8.61 \text{ mm}^3$ at follow-up ($p = 0.41$) (see online supplemental table 1).

After 28 days, 100% patency was observed in the vital and elastase groups with or without ASA and in the decellularized group with ASA. Complete thrombosis of the aneurysm and the parent artery was observed in three (50%) of six animals in the decellularized group without ASA. Partial thrombosis was observed in three of six aneurysms in the decellularized group without ASA, in one (16%) of six aneurysms in both the vital group with ASA and the elastase group without ASA, and in all six aneurysms in the decellularized group with ASA. Complete and partial thrombosis of the aneurysm was visualized by contrast-enhanced MRI followed by fluorescence angiography.

Follow-up histological findings

Histological grading included periadventitial inflammation, aneurysm wall inflammation, neutrophils in the thrombus, and periadventitial fibrosis (figure 3).

ASA significantly reduced periadventitial inflammation in the vital, decellularized, and elastase groups ($p < 0.01$) (figures 3 and 4). Likewise, ASA also significantly reduced aneurysm wall inflammation in the vital ($p < 0.01$), decellularized ($p < 0.05$), and elastase ($p < 0.01$) groups (figures 3 and 4). However, ASA did not significantly reduce neutrophils in the thrombus in the vital, decellularized, or elastase groups. Invasion of neutrophils

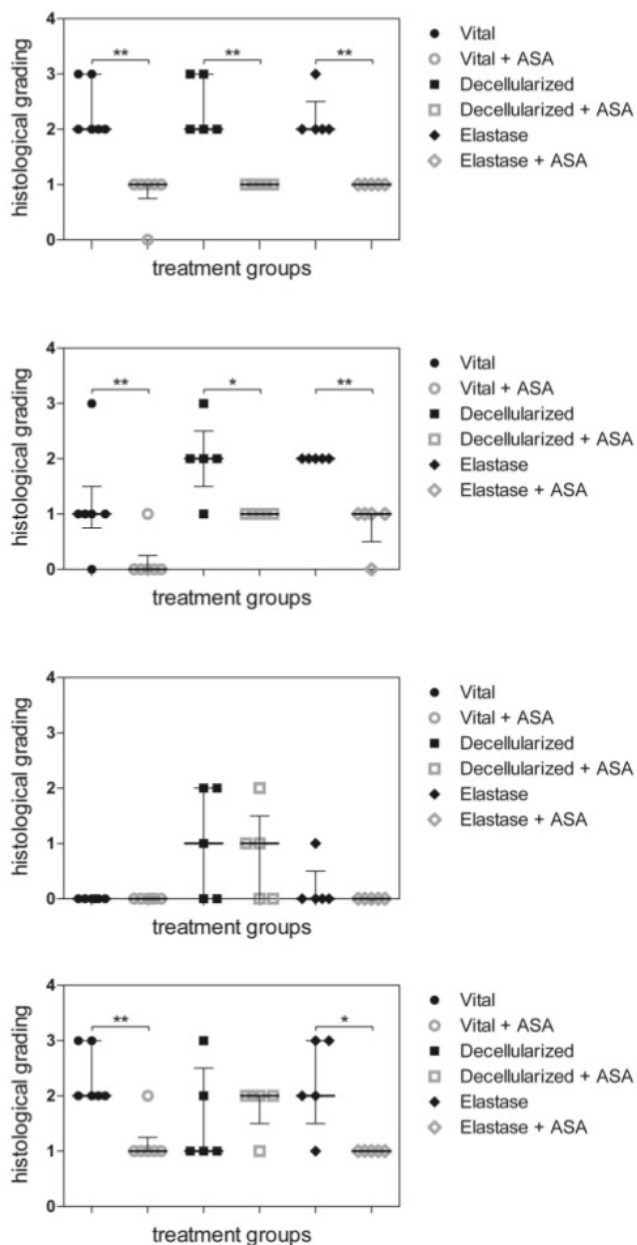


Figure 3 . Bar graph depicting histological grading for periaortic inflammation, aneurysm wall inflammation, neutrophils in the thrombus and periaortic fibrosis. Analyses are grouped for vital, decellularized, and elastase-treated aneurysms without and with ASA treatment using a previously described 4-point grading system (0 = none, 1 = mild, 2 = moderate, 3 = severe). * $p < 0.05$, ** $p < 0.01$ vs. corresponding group. (A) Periaortic inflammation. ASA intake significantly reduced periaortic inflammation in the vital, decellularized, and elastase groups. (B) Aneurysm wall inflammation. ASA intake significantly reduced aneurysm wall inflammation in the vital, decellularized, and elastase groups. (C) Neutrophils in the thrombus. ASA intake did not significantly reduce neutrophils in the thrombus in the vital, decellularized, or elastase groups. However, a pronounced thrombus invasion of neutrophils was observed in the decellularized group compared with vital and elastase groups. (D) Periaortic fibrosis. ASA intake significantly reduced periaortic fibrosis in the vital and elastase groups but not in the decellularized group.

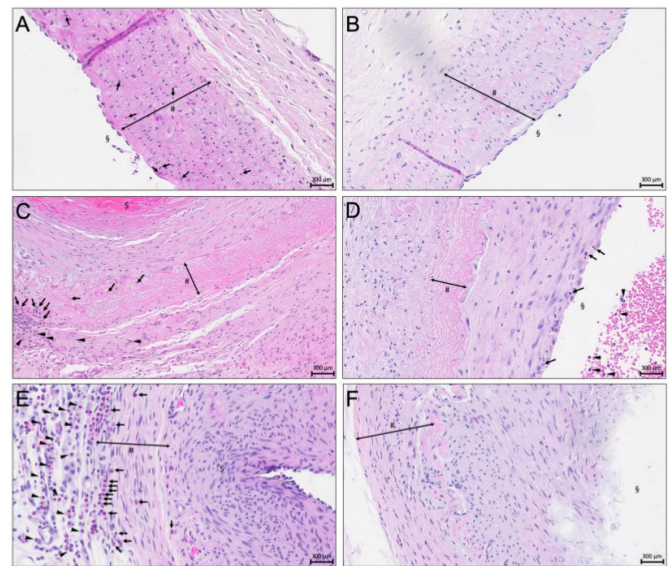


Figure 4 . Representative microphotographs of vital, decellularized, and elastase-treated aneurysms without and with ASA treatment. Hematoxylin-eosin (HE) staining of the media (#). Scale bar: 300 μ m.

(A) Vital aneurysm without ASA treatment. Aneurysm lumen (§), infiltration of granulocytes (Black arrows).

(B) Vital aneurysm with ASA treatment shows no sign of wall inflammation or periaortic inflammation. Aneurysm lumen (§).

(C) Decellularized aneurysm without ASA treatment. Note the apical thrombus formation (§), and intense inflammation of aneurysm wall and periaortic characterized by accumulating granulocytes (black arrows). Periaortic tissue layer (black arrowheads).

(D) Decellularized aneurysm with ASA pretreatment shows no signs of inflammation of aneurysm wall (#) or periaortic. Note luminal thrombus formation and sparse neutrophils in the outer luminal layer of the thrombus (black arrows) and intraluminally (black arrowheads). Aneurysm lumen (§).

(E) Elastase-treated aneurysm without ASA. Beginning luminal thrombus formation (§) with excessive infiltration of neutrophil granulocytes in the aneurysm wall (black arrows and highly degenerated extracellular matrix). Note excessive periaortic inflammation (black arrow heads).

(F) Elastase-treated aneurysm with ASA. Note the highly degenerated matrix in the aneurysm wall. Note absence of inflammation in aneurysm wall and periaortic. Lumen of the aneurysm (§).

was pronounced in the decellularized group compared with the vital and elastase groups (figure 3). Periaortic fibrosis was significantly reduced in the vital ($p < 0.01$) and elastase groups ($p < 0.05$) and was more pronounced in the vital group (figure 3).

Among grading for other histological characteristics (online supplemental figure 4), we noted that, in all six groups, neither hematoma nor dissection affected the aneurysm wall, endothelial cellularity was not significantly altered, and no significant differences developed in neointima formation. Luminal thrombosis was more pronounced in both decellularized groups. In the vital and elastase groups, neointima formation could not be

detected compared with the decellularized groups in which a stronger tendency to neointima formation was noted with ASA (see online supplemental figures 5-7 for illustrative histological samples).

General data and surgical characteristics

Of a total of 45 animals used in the experiments, 14 (4 vital, 1 decellularized, 9 elastase) were used in a pilot study to establish reliable and consistent reproducible procedures. Of 36 animals included in the final study, no deaths occurred intraoperatively and no ischemic brain lesions were detected by MRI in any rabbit before euthanasia.

Among nine (20%) animals that died prematurely and were excluded from analysis, two had complete thrombosis of the left parent artery on postoperative days 3 and 7; three had neurologic worsening and were euthanized postoperatively on days 4, 5, and 8; one had intraoperative digestion of the left carotid artery and was subsequently euthanized; and three died in their cages of unknown causes postoperatively on days 2, 7, and 11.

Intraoperatively, 10 (23%) of 44 aneurysms showed no contrast enhancement in the arterial pouch on fluorescence angiography. These 10 aneurysms then underwent reclamping, reopening, and flushing with heparinized saline followed by thrombus evacuation. Repeat fluorescence video angiography confirmed patency in all 44 aneurysm cases. Physiological values and amplitude of blood pressure were measured in the auricular artery after reopening all vascular clamps.

Follow-up MRI patency rate

After 28 days, 33 (92%) of 36 of aneurysms remained open, two (6%) had complete thrombosis of the aneurysm and its parent vessel complex, and one had complete aneurysm thrombosis. Partial aneurysm thrombosis was observed in 11 (31%) aneurysms, especially among nine (25%) in the decellularized group (online supplemental table 1).

DISCUSSION

This experimental study studied the effects of ASA on bifurcation aneurysms in a rabbit model, specifically the natural course of inflammation and aneurysm growth in groups defined by wall characteristics as vital, decellularized, or elastase degraded. Our results of continuous ASA intake found significantly decreased aneurysm growth in vital aneurysms, mimicking early aneurysmal disease, as well as decreased inflammation in the periadventitia and aneurysm wall irrespective of any of the three initial wall conditions. Interestingly, ASA intake did not attenuate aneurysm growth in elastase-pretreated pouches. The protective effect of ASA in the early stage of aneurysm might be lost in progressive aneurysmal disease.

Vital aneurysms

To analyze potential effects of ASA in the early phase of aneurysm formation, vital arterial pouches were implanted in an artificial arterial bifurcation. Compared with the control group, ASA significantly prevented aneurysm growth and, in histological studies, significantly reduced aneurysm wall inflammation, periadventitial inflammation, and fibrosis.

The potential role of ASA in preventing intracranial aneurysm growth and rupture is multifold.⁶ First, it acts to block COX-2, which is associated with intracranial aneurysm formation and rupture. Hasan *et al* showed upregulation of PGES-1 and COX-2 in histological specimens of human ruptured intracranial aneurysms compared with unruptured intracranial aneurysms.⁵

In tissue samples of patients who underwent intracranial aneurysm clipping, attenuated expressions of PGES-1, COX-2, and macrophages were detected in the wall after 3 months of ASA therapy compared with the control group without ASA. As shown by novel imaging protocols, aneurysm wall inflammation was reduced in patients who received continuous ASA treatment prior to elective clipping.¹⁰ With regard to these issues, a vessel wall oriented therapy with ASA might provide an interesting future approach in identifying patients at high risk for intracranial aneurysm rupture and/or assessing treatment response.

Decellularized aneurysms

Decellularized aneurysms did not show significant enlargement with or without ASA treatment. Compared with the control group, inflammation in the aneurysm wall and periadventitia was significantly reduced in the ASA arm. The role and importance of degenerated aneurysm walls in growth and rupture is undisputed.^{4,16} In general, fewer mural cells implicate a worse biologic response in aneurysm healing because of the inability of intraluminal thrombus to organize. Previously, loss of mural cells was shown to have an important role in furthering its progression in a saccular rat sidewall model with untreated aneurysms,⁴ after coil embolization,¹⁷ and also after stent treatment.¹⁸ With decreased numbers, there are fewer cells that can migrate into the thrombus and form a neointima. Furthermore, in a sidewall rabbit model, all aneurysms thrombosed spontaneously.¹⁹ In our bifurcation series, in the ASA arm all aneurysms had partial thrombosis whereas the group without ASA had complete thrombosis in half of the aneurysms and partial thrombosis in the other half. Graft decellularization by SDS, including endothelial cells, may have contributed substantially to this high rate of thrombosis. Therefore, other degradative compounds such as elastase pretreatment were further analyzed for a potential ASA effect on aneurysm formation in advanced disease.

Elastase-degraded aneurysms

Compared with vital aneurysms, a protective effect in prevention of aneurysm growth was not observed in elastase-degraded pouches and ASA intake clearly failed to prevent aneurysm growth. After 28 days, significant growth was observed both with and without ASA. Therefore, while ASA intake might be protective during early stages of aneurysm formation with relatively healthy vessel walls, this protective effect is likely to be lost in advanced disease. Nevertheless, aneurysm wall inflammation, periadventitial inflammation, and fibrosis were significantly reduced in the ASA group. This fact suggests that, along with inflammatory components, other factors driving aneurysm enlargement (eg, hemodynamics of a true vessel bifurcation) must also be considered.

In our pilot study using 14 animals, the group of nine elastase-treated animals was the largest; this group also included 5/9 animals that died prematurely and contributed to the overall 15.3% mortality rate. The reasons for the increased mortality, even when performing topical elastase incubation in our model, might be the non-specific effects of elastase in circumferential digestion of all tissues (shown in online supplemental figure 2C), leading to possible thrombogenic reactions at a molecular level.²⁰

Use of ASA in aneurysm treatment and further clinical implications

Several studies have previously shown substantial increases in aneurysm size in deteriorated aneurysm walls in rabbits over time when using adjuncts such as Eastman 910 or elastase after

in vitro collagenase I infusion.²¹ In our bifurcation series, these observations were confirmed in both vital and elastase-degraded pouches. The significant aneurysm growth over time observed in the vital group without ASA treatment was similar to the natural course of bifurcation aneurysms observed in humans.² Here, the significant upregulation of neutrophils in the periadventitia and aneurysm wall might be the cause. Accordingly, with its anti-inflammatory effects, ASA pretreatment in the vital group thus prevented significant aneurysm growth after 28 days. Aligned with the results of other studies, we consider that, through antagonizing inflammatory processes such as COX-2 and PGES-1 inhibition, a certain degree of aneurysm wall stabilization might be achieved.

In a retrospective review of 146 patients, Zanaty *et al* observed that ASA intake significantly decreased the rate of intracranial aneurysm growth over time.¹² In a large retrospective single-center study of 4701 patients, Can *et al* found that ASA intake was associated with a decreased risk of intracranial aneurysm rupture.²² Furthermore, Hudson *et al* clearly demonstrated that ASA intake beneficially modulated the inflammatory microenvironment within the intracranial aneurysm vessel wall, thereby preventing rupture and aneurysm growth in patients with multiple intracranial aneurysms over time.⁸ These findings were confirmed in other preclinical and clinical investigations.^{23,24}

Comparable with our results, preclinical and clinical studies have reported similar encouraging results when targeting inflammatory processes in the aneurysm wall, especially with ASA, to avoid further growth and rupture; they also hypothesized that its anti-inflammatory effect might be protective in providing aneurysm stability.^{3,10} More recently, these data were further confirmed in population-based studies of more than 200 000 patients with intracranial aneurysms who received low-dose long-term ASA therapy. Regarding the entire study population, the incidence of subarachnoid hemorrhage by aneurysm rupture was reduced by more than 20%.²⁵ Nonetheless, the benefit of this conservative treatment approach must be confirmed in prospective randomized multicenter trials such as the PROTECT-U trial, which considered the influences of blood pressure reduction in combination with ASA.¹

Study limitations

To the best of our knowledge, this study is the first report of a true bifurcation aneurysm model using arterial grafts that allow for a direct comparison of different wall characteristics (vital, decellularized, elastase degraded). Strengths of this model included its relatively large sample size and a multimodal data analysis approach (ie, baseline and follow-up fluorescence angiography, MRI, histological assessment) that provided consistent and reliable values for results and interpretation.

The aim of these experiments was to study a biological concept of vessel wall biology, therefore the results of this extracranial aneurysm model should be extrapolated with caution to a true intracranial aneurysm model. Compared with endovascular approaches for aneurysm induction, surgical dissection causes locoregional inflammation so a surgically-created aneurysm likely causes stronger long-lasting inflammation. To reduce this bias in analyzing the data as far as possible, the final follow-up timepoint was 28 days after surgical creation of the aneurysm. Furthermore, postoperative administration of meloxicam for analgesia may have influenced locoregional inflammation in a beneficial fashion. However, this bias was minimized because all the animals received meloxicam for only 3 days. Regarding the 20% mortality and initial 23% rate of intraoperative thromboses verified by fluorescence angiography, other factors to consider

include potential thrombogenic properties of the suture material and modified arterial pouches, and the learning curve required for this sophisticated surgical technique. Of note, initial MRI directly after implanting the arterial pouch would provide the most precise aneurysm volume, but partial thrombosis of the arterial pouch within 28 days detected by terminal MRI might potentially not depict true aneurysm growth over time and could even interfere in the comparison between immediate postoperative MRI and MRI performed at terminal follow-up. Lastly, immediate postoperative MRI was not performable because of missing availability, so exact macroscopic measurement was performed every time prior to implantation and also after terminal MRI and explanation of the aneurysm complex to detect macroscopic pattern of growth. Therefore, a certain reproducibility should be given but, nevertheless, macroscopic measurement after pouch implantation intraoperatively as well as postoperatively after 28 days would eventually be more precise.

Besides the use of neutrophils to monitor the indirect effects of ASA on the inflammatory microenvironment, many specific parameters (eg, COX-1, COX-2) can now be measured to identify direct effects. Nevertheless, previous studies have identified neutrophils as the driving factors for aneurysm growth. Potential molecular targets of ASA in cerebral aneurysm pathophysiology are manifold. For example, prostaglandin E2 targeted by ASA increases vascular permeability and attracts/activates both macrophages and neutrophils. Therefore, an indirect effect of ASA intake should be at least depicted.

Finally, although we aimed for maximal standardization, we cannot exclude the possibility that slight differences in aneurysm volumes might have been hemodynamically relevant by causing different shear stress.

CONCLUSIONS

We believe this to be the first report of a true bifurcation aneurysm model using arterial grafts that allowed for a direct comparison of different wall characteristics (vital, decellularized, elastase-degraded). Continuous ASA administration reduced inflammation of the aneurysm wall irrespective of the initial wall condition in a rabbit true bifurcation aneurysm model. ASA significantly prevented aneurysm growth in aneurysms with vital walls, whereas this preventive effect did not seem to play an important role in elastase-degraded pouches. Considering these findings, the potential preventive effect of ASA in the early phase of aneurysm formation in patients with healthy vessels may be lost in those with highly degenerative aneurysm walls.

Acknowledgements We are deeply grateful to: Olgica Beslac and Kay Nettelbeck for their excellent support and technical assistance during the peri-operative phase; Alessandra Bergadano, DVM, PhD, for the dedicated supervision of the long-term animal health and Mary Kemper for editing and proofreading.

Contributors Conception and design: SW, SM. Experimental procedures: SW, SM, BEG, FS. Histological sample preparation and analysis: SW, HRW, MvG, GB, LA, SS. Drafting the article: SW, BEG, SM. Statistical analysis and interpretation of data: SW, BEG, LA, SM. Critically revising the article: JF, HRW, SM, LR, BEG, JR, DC. Administrative support: SM.

Funding This work was supported by the Swiss National Science Foundation SNF (310030_182450). The authors are solely responsible for the design and conduct of the presented study and declare no competing interests.

Competing interests None declared.

Patient consent for publication Not required.

Ethics approval The project has been performed according to the Animal Research: Reporting of In Vivo Experiments (ARRIVE) guidelines and was performed in accordance with the National Institutes of Health Guidelines for the care and use of experimental animals and with the approval of the Animal Care Committee of the Canton Bern, Switzerland (Approval No. BE 108/16).

Provenance and peer review Not commissioned; externally peer reviewed.

Data availability statement All data relevant to the study are included in the article or uploaded as supplementary information.

Supplemental material This content has been supplied by the author(s). It has not been vetted by BMJ Publishing Group Limited (BMJ) and may not have been peer-reviewed. Any opinions or recommendations discussed are solely those of the author(s) and are not endorsed by BMJ. BMJ disclaims all liability and responsibility arising from any reliance placed on the content. Where the content includes any translated material, BMJ does not warrant the accuracy and reliability of the translations (including but not limited to local regulations, clinical guidelines, terminology, drug names and drug dosages), and is not responsible for any error and/or omissions arising from translation and adaptation or otherwise.

Open access This is an open access article distributed in accordance with the Creative Commons Attribution Non Commercial (CC BY-NC 4.0) license, which permits others to distribute, remix, adapt, build upon this work non-commercially, and license their derivative works on different terms, provided the original work is properly cited, appropriate credit is given, any changes made indicated, and the use is non-commercial. See: <http://creativecommons.org/licenses/by-nc/4.0/>.

ORCID iDs

Stefan Wanderer <http://orcid.org/0000-0002-4510-5741>

Basil Erwin Grüter <http://orcid.org/0000-0002-6314-2482>

Serge Marbacher <http://orcid.org/0000-0001-6305-7571>

REFERENCES

- Vergouwen MDI, Rinkel GJ, Algra A, *et al.* Prospective randomized open-label trial to evaluate risk factor management in patients with unruptured intracranial aneurysms: study protocol. *Int J Stroke* 2018;13:992–8.
- Molyneux AJ, Kerr RSC, Yu L-M, *et al.* International Subarachnoid Aneurysm Trial (ISAT) of neurosurgical clipping versus endovascular coiling in 2143 patients with ruptured intracranial aneurysms: a randomised comparison of effects on survival, dependency, seizures, rebleeding, subgroups, and aneurysm occlusion. *Lancet* 2005;366:809–17.
- Hasan DM, Mahaney KB, Brown RD, *et al.* Aspirin as a promising agent for decreasing incidence of cerebral aneurysm rupture. *Stroke* 2011;42:3156–62.
- Marbacher S, Marjamaa J, Bradacova K, *et al.* Loss of mural cells leads to wall degeneration, aneurysm growth, and eventual rupture in a rat aneurysm model. *Stroke* 2014;45:248–54.
- Hasan D, Hashimoto T, Kung D, *et al.* Upregulation of cyclooxygenase-2 (COX-2) and microsomal prostaglandin E2 synthase-1 (mPGES-1) in wall of ruptured human cerebral aneurysms: preliminary results. *Stroke* 2012;43:1964–7.
- Starke RM, Chalouhi N, Ding D, *et al.* Potential role of aspirin in the prevention of aneurysmal subarachnoid hemorrhage. *Cerebrovasc Dis* 2015;39:332–42.
- Chalouhi N, Atallah E, Jabbour P, *et al.* Aspirin for the prevention of intracranial aneurysm rupture. *Neurosurgery* 2017;64:114–8.
- Hudson JS, Marincovich AJ, Roa JA, *et al.* Aspirin and intracranial aneurysms. *Stroke* 2019;50:2591–6.
- Hasan DM, Chalouhi N, Jabbour P, *et al.* Imaging aspirin effect on macrophages in the wall of human cerebral aneurysms using ferumoxytol-enhanced MRI: preliminary results. *J Neuroradiol* 2013;40:187–91.
- Hasan DM, Chalouhi N, Jabbour P, *et al.* Evidence that acetylsalicylic acid attenuates inflammation in the walls of human cerebral aneurysms: preliminary results. *J Am Heart Assoc* 2013;2:e000019.
- Roa JA, Zanaty M, Ishii D, *et al.* Decreased contrast enhancement on high-resolution vessel wall imaging of unruptured intracranial aneurysms in patients taking aspirin. *J Neurosurg* 2020;902–8.
- Zanaty M, Roa JA, Nakagawa D, *et al.* Aspirin associated with decreased rate of intracranial aneurysm growth. *J Neurosurg* 2019:1–8.
- Grüter BE, Täschler D, Rey J, *et al.* Fluorescence video angiography for evaluation of dynamic perfusion status in an aneurysm preclinical experimental setting. *Oper Neurosurg* 2019;17:432–8.
- Kilkenny C, Browne W, Cuthill IC, *et al.* Animal research: reporting in vivo experiments: the ARRIVE guidelines. *Br J Pharmacol* 2010;160:1577–9.
- Wanderer S, Waltenspuel C, Grüter BE, *et al.* Arterial pouch microsurgical bifurcation aneurysm model in the rabbit. *J Vis Exp* 2020;159. doi:10.3791/61157. [Epub ahead of print: 14 May 2020].
- Frösen J. Smooth muscle cells and the formation, degeneration, and rupture of saccular intracranial aneurysm wall—a review of current pathophysiological knowledge. *Transl Stroke Res* 2014;5:347–56.
- Nevezati E, Rey J, Coluccia D, *et al.* Aneurysm wall cellularity affects healing after coil embolization: assessment in a rat saccular aneurysm model. *J Neurointerv Surg* 2020;12:621–5.
- Grüter BE, Täschler D, Strange F, *et al.* Testing bioresorbable stent feasibility in a rat aneurysm model. *J Neurointerv Surg* 2019;11:1050–4.
- Grüter BE, Wanderer S, Strange F, *et al.* Comparison of aneurysm patency and mural inflammation in an arterial rabbit Sidewall and bifurcation aneurysm model under consideration of different wall conditions. *Brain Sci* 2020;10:197.
- Marbacher S, Strange F, Frosen J, *et al.* Preclinical extracranial aneurysm models for the study and treatment of brain aneurysms: a systematic review. *J Cereb Blood Flow Metab* 2020;271678X:20908363.
- Troupp H, Rinne T. Methyl-2-cyanoacrylate (Eastman 910) in experimental vascular surgery with a note on experimental arterial aneurysms. *J Neurosurg* 1964;21:1067–9.
- Can A, Rudy RF, Castro VM, *et al.* Association between aspirin dose and subarachnoid hemorrhage from saccular aneurysms: a case-control study. *Neurology* 2018;91:e1175–81.
- Fisher CL, Demel SL. Nonsteroidal anti-inflammatory drugs: a potential pharmacological treatment for intracranial aneurysm. *Cerebrovasc Dis Extra* 2019;9:31–45.
- Suzuki T, Kamio Y, Makino H, *et al.* Prevention effect of antiplatelets on aneurysm rupture in a mouse intracranial aneurysm model. *Cerebrovasc Dis* 2018;45:180–6.
- Cea Soriano L, Gaist D, Soriano-Gabarró M, *et al.* Low-dose aspirin and risk of intracranial bleeds: an observational study in UK general practice. *Neurology* 2017;89:2280–7.

Supplementary Materials

Supplementary Methods

Intraoperative heparin administration. Twice during surgery, the activated clotting time (ACT) was measured to titrate heparin administration. The two points included first, before ligation of the right proximal CCA and during administration of heparin (Heparin Bichsel AG, Switzerland) bolus 500 international units (IU)/kg, and second after reopening all arterial clamps.

Arterial wall degradation protocols. Arterial pouches from a donor animal (allografts from both CCAs) were decellularized in 1% SDS for 6 hours at 37° C. Until ready for use, decellularized donor grafts were stored in phosphate-based saline buffer (0.1 molar) at a potential hydrogenii from 7.4 at -70° C. For elastase degradation, the arterial pouch (autograft from the right CCA) was meticulously cleaned from soft tissue intraoperatively, incubation with 100 Units porcine elastase (Sigma Aldrich, Nr. 45124/45125, Switzerland) dissolved in 5 milliliter (ml) TRIS-Buffer (Sigma Aldrich, Nr. 93302, Switzerland) followed on the day of the experiment for 20 minutes with gentle shaking at room temperature.

Anesthesia protocol. Rabbits were sedated with ketamine (Narketan 100 mg/ml, Vétoquinol, Germany) 20 mg/kg sc, dexmedetomidine 100 mcg/kg (Dexdomitor 0.5 mg/ml, Orion Pharma, Finland) and methadone 0.3 mg/kg (Methadon Streuli, 10 mg/ml, Streuli pharma, Switzerland), and left undisturbed for 10-15 minutes. Once sedation was adequate, oxygen supplementation via face-mask was started and continued until tracheal intubation was performed. A venous catheter and arterial catheter were placed, respectively, in the auricular vein and in the

contralateral auricular artery. For anesthesia induction and tracheal intubation, propofol (Propofol 1% MCT Fresenius, Fresenius Kabi, Germany) 1-3 mg/kg intravenously (iv) was administered to effect. Tracheal intubation was performed with a silicone endotracheal tube (internal diameter 3 mm), which was then connected to a low-resistance pediatric rebreathing system and ventilation mode (spontaneous, not mechanical) was individually selected to avoid uncontrolled hypercapnia ($\text{PaCO}_2 \geq 55$ mmHg). Unawareness was maintained with isoflurane (Isofluran Baxter AG, Switzerland) in 100% oxygen targeting an end tidal of 1.8 %. A forced-air warming device was used to ensure normothermia. Intraoperative monitoring consisted of the following: rectal temperature, ECG (II lead), pulse oxymetry, inspired and expired gas, spirometry, invasive blood pressure, and indexed EEG (bispectral index). Balanced analgesia was provided using perineuraxial infiltration of ropivacaine (Ropivacain 2 mg/ml, Fresenius Kabi, Switzerland) 0.75% 2-3 mg/kg before surgery. Intraoperative analgesia consisted of continuous rate infusion (CRI) of lidocaine (Lidocaine 1% HCl, Streuli Pharma, Switzerland) 50 mcg/kg/min and fentanyl (Fentanyl 50 mg/ml, Janssen, Belgium) (3-10 mcg/kg/h). Fluid therapy was administered from induction of general anesthesia until rabbits recovered sternal recumbency and consisted of Ringer lactate 3-5 ml/kg/h.

Postoperative care. When the rabbit regained spontaneous swallowing, tracheal extubation was performed. This was followed by administration of meloxicam (Metacam 5 mg/ml, Boehringer Ingelheim, Switzerland) 0.5 milligram (mg)/kilogram (kg) intravenously (iv), ASA 10 mg/kg iv, vitamin B₁₂ (Vitarubin, Streuli Pharma, Switzerland) 100 mcg subcutaneously (sc), and amoxicillin and clavulanic acid (Clamoxyl 250 mg, Glaxo Smith AG, Switzerland) 20 mg/kg iv. Supplemental

oxygen via face mask was delivered until the rabbits regained spontaneously sternal recumbency. Normothermia was ensured by a forced-air warming device.

Pain scoring and postoperative follow-up care were performed for 3 days in accordance with the guidelines for the assessment and management of pain in rodents and rabbits. Postoperative analgesia consisted of meloxicam for 3 days sc and a fentanyl patch (Durogesic 12 mcg/h, Janssen, Belgium) placed on the outer ear for 72 hours. As rescue analgesia, an injection of methadone (Methadon Streuli, 10 mg/ml, Streuli Pharma, Switzerland) 0.2 mg/kg was planned. For the ASA group, 500 mg powder (Sanofi-Aventis, Switzerland) was dissolved in the drinking water until the day of the final MRI. Low molecular weight heparin (250 IU/kg) for all groups was administered for 3 days.

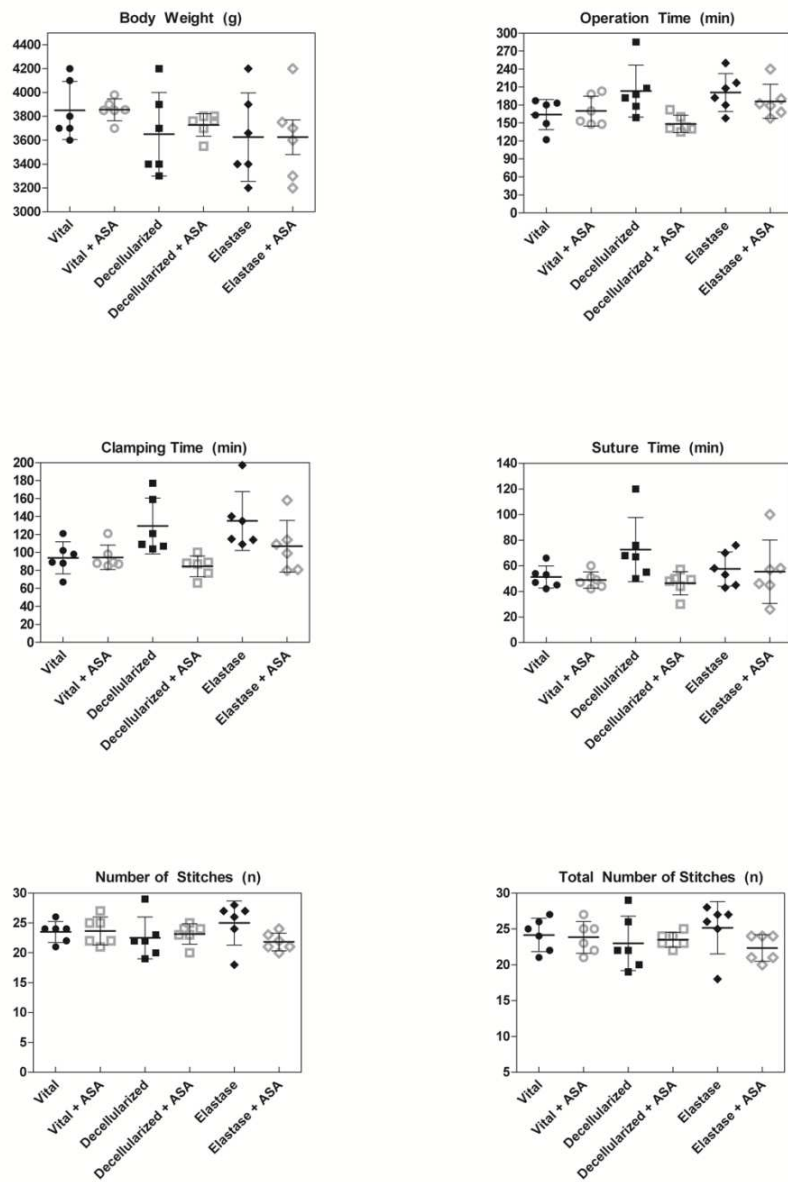
MRI protocol. Prior to MRI, 2 peripheral venous accesses (marginal auricular veins) were established in each rabbit. Following premedication (see Methods in paper) and transport, ketamine 15 mg/kg and medetomidine (Domitor, 1 mg/ml, Vétoquinol, Germany) 0.1 mg/kg were injected intramuscularly or subcutaneously prior to MRI, according to the individual awareness after premedication. Ten to 20 minutes after injection, ketamine CRI (5mg/kg/h) was started: dosage was adapted to guarantee immobility and unawareness with progressive increases up to 15 mg/kg. The CRI was preceded by an intravenous bolus of ketamine 1-3 mg/kg if unawareness was not achieved with the combination of ketamine-medetomidine. Imaging sequences acquired on a 3 T Magnetom Skyra (Siemens) included T2 space sagittal, T2 dark fluid fs sagittal, transversal DWI, transversal T1 fs, TOF angiography, neck angiography with contrast enhancement, T1 mprage sagittal fs with contrast enhancement, and transversal T1 fs.

Histological Grading System. Characteristics assessed and scored included: Periadventitial inflammation (0 = none, 1 = mild, 2 = moderate, 3 = severe); periadventitial fibrosis (0 = none, 1 = mild, 2 = moderate, 3 = severe); aneurysm wall inflammation (0 = none, 1 = few (1-3) spots, 2 = many (>4) spots, 3 = ubiquitous); aneurysm wall hematoma (0 = none, 1 = few (1-3) spots, 2 = many (>4) spots, 3 = ubiquitous); aneurysm wall cellularity (0 = none, 1 = few (1-3) spots, 2 = many (>4) spots, 3 = ubiquitous); aneurysm wall dissection (0 = none, 1 = few (1-3) spots, 2 = many (>4) spots, 3 = ubiquitous); endothelial cellularity (0 = none, 1 = few (1-3) spots, 2 = many (>4) spots, 3 = ubiquitous); luminal thrombus (0 = absent, 1 = present); neutrophils in the thrombus (0 = none, 1 = mild, 2 = moderate, 3 = severe); and neointima formation (0 = none, 1 = organizing thrombus, 2 = organizing thrombus and neointima formation, 3 = mature neointima). Scores were dichotomized as (1) (none/mild) and moderate/severe; (2) no/few cells and focal hypo-cellularity/normal cell count; and (3) no neointima/organizing thrombus and organizing neointima/mature neointima.

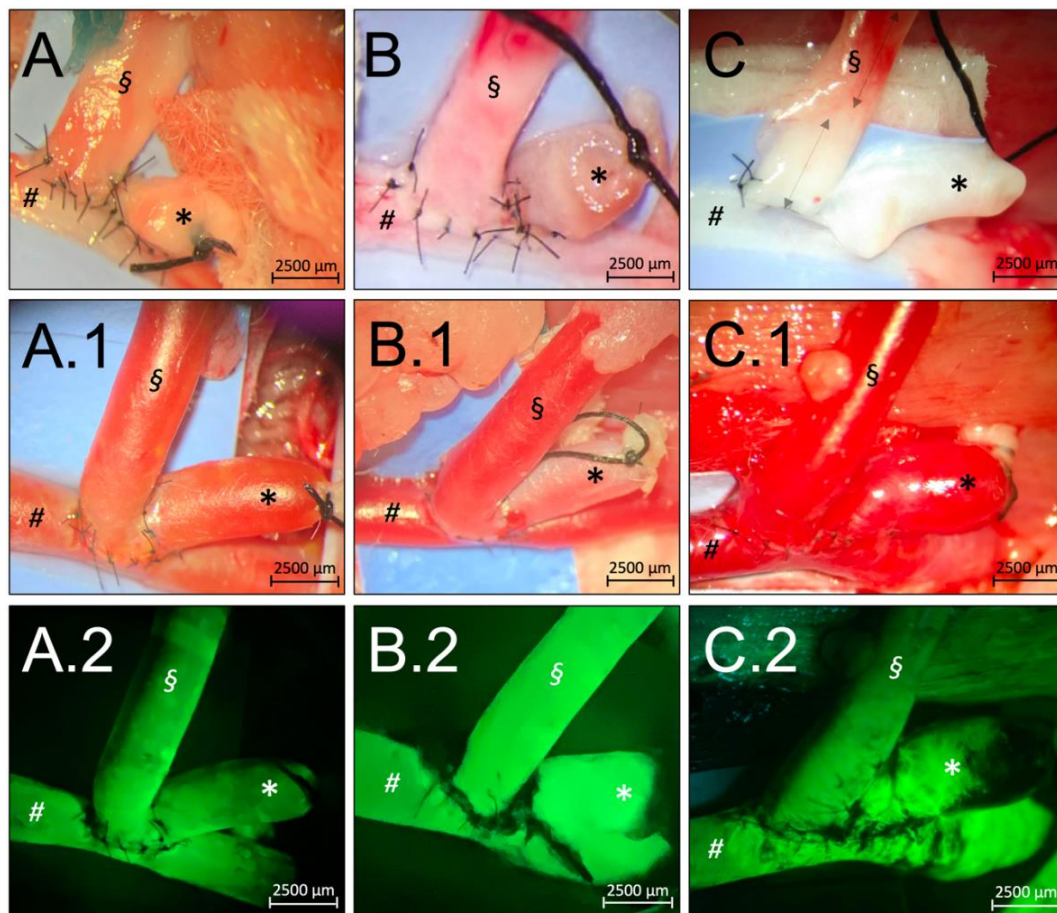
Supplementary Figures

Supplementary Figure 1. Bar charts for surgical characteristics. Body weight in gram.

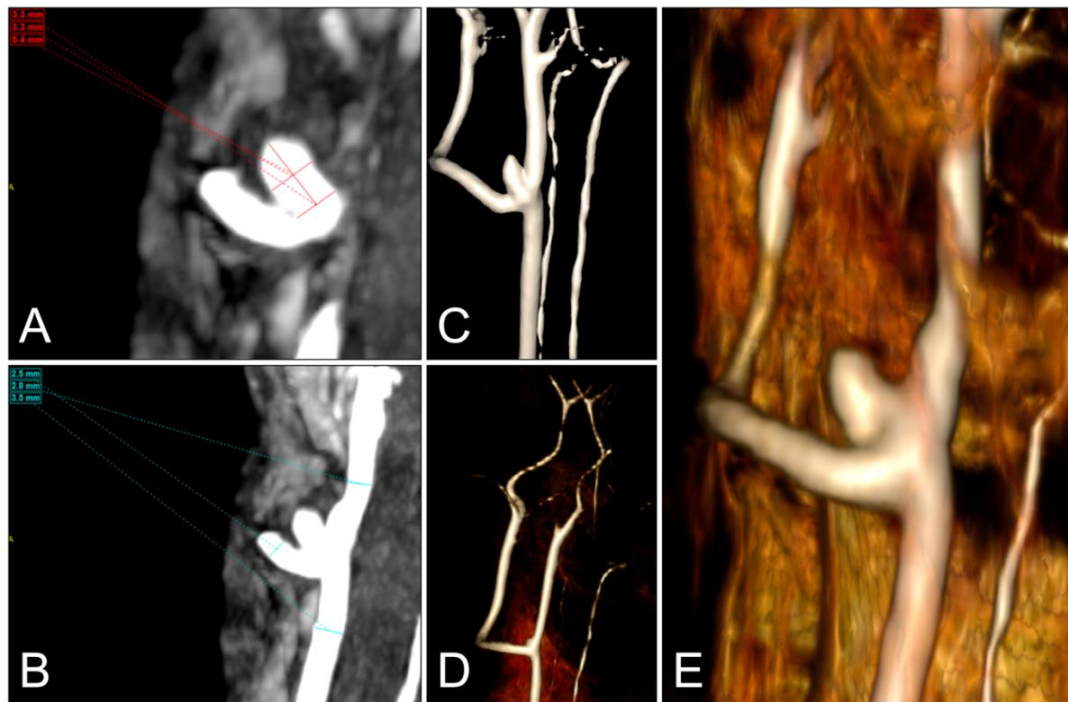
Clamping, operation, and suture times in minutes. Total number of stitches includes stitches and restitches because of an initial insufficient anastomosis.



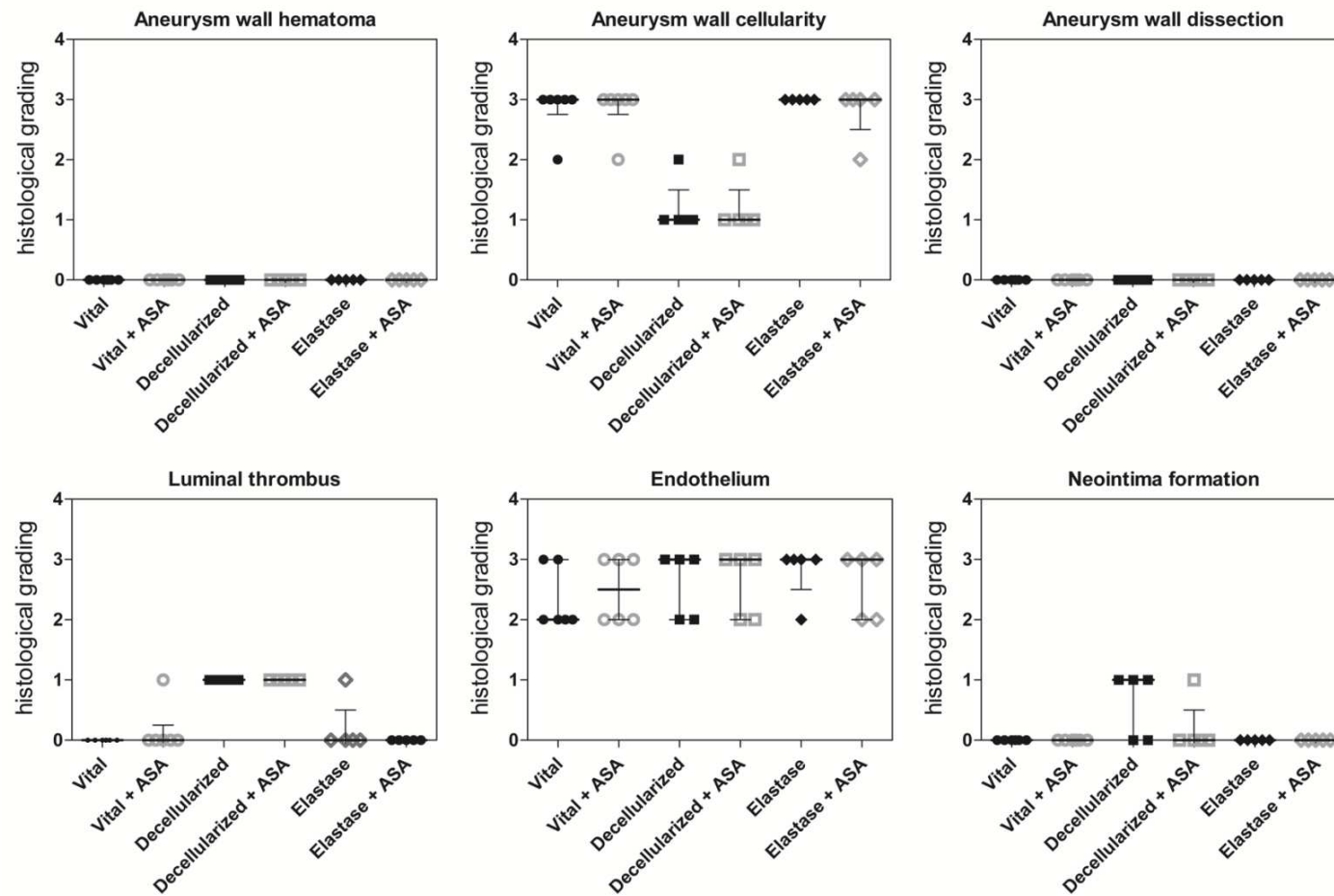
Supplementary Figure 2. Photographs illustrating the macroscopic findings. Intraoperative situs upon aneurysm creation of vital, (A) decellularized (B), and elastase-degraded (C) vessel pouches. Intraoperative macroscopic findings after opening the arterial clamp show aneurysm perfusion in vital (A.1), decellularized (B.1), and elastase-degraded aneurysms (C.1). Intraoperative flow assessment after administration of fluorescein in vital (A.2), decellularized (B.2), and elastase-degraded (C.1) aneurysms. Legend: § right CCA, # left CCA, * aneurysm pouch. Note: (1) dotted and non-dotted arrows in (C) show the aggressive co-effect of elastase preincubated pouches on the angioarchitecture pronounced proximally to the anastomosis. (2) kinking of the elastase-degraded pouch in (C.1) compared to decellularized (B.1) and vital pouches (A.1).



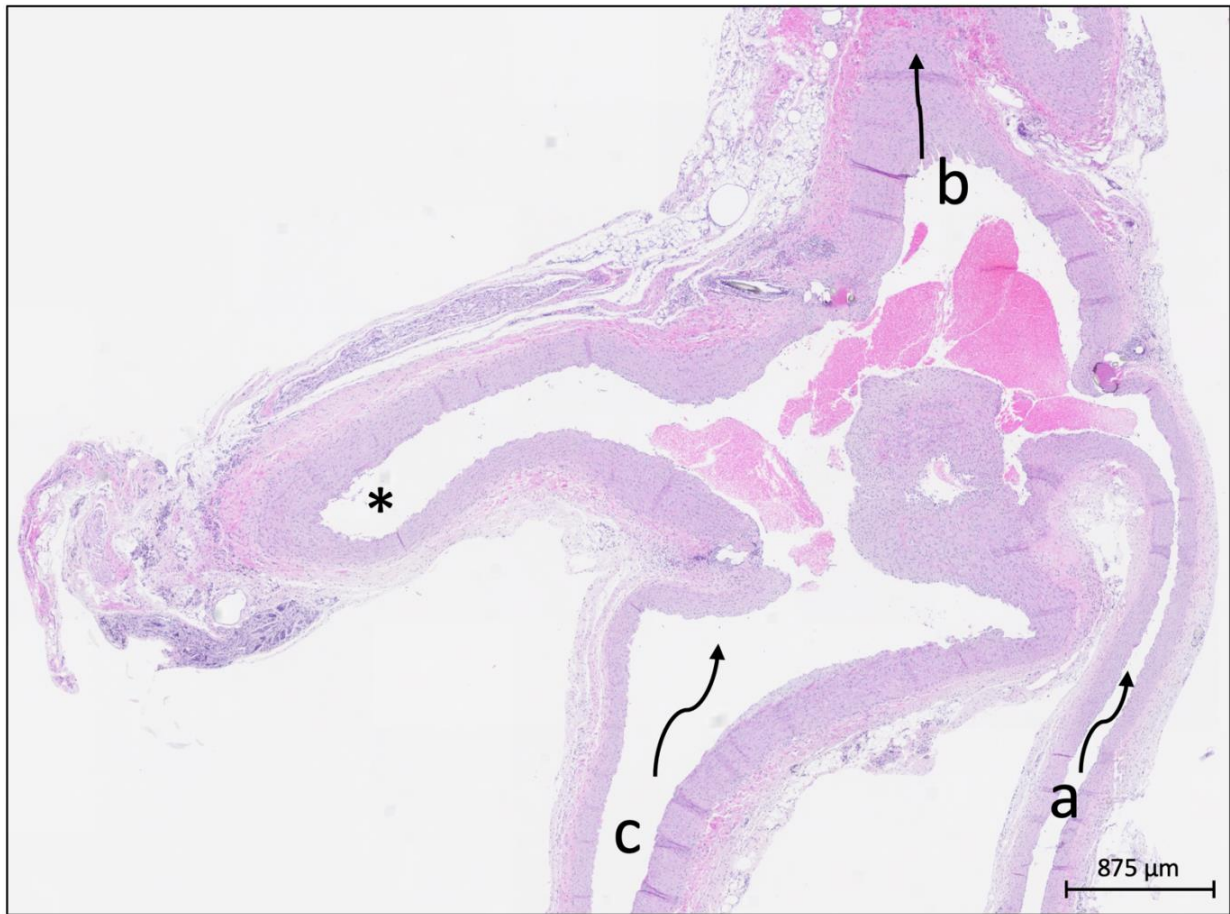
Supplementary Figure 3. Illustrative panel of MR Angiography including CE-3D-MRA-morphometric measurements. Example of maximum intensity projections (8.5) of a vital arterial pouch aneurysm at 28-day follow-up. (A) Measurement of aneurysm height, width and depth. (B) Diameter of the corresponding parent arteries in the sagittal view. (C-E) show 3D-MRA reconstructions of vital, decellularized and elastase-degraded arterial pouches, respectively.



Supplementary Figure 4. Detailed histological grading. Comparison of various parameters in the vital, decellularized, and elastase-degraded groups without and with ASA treatment (0 = none, 1 = mild, 2 = moderate, 3 = severe).

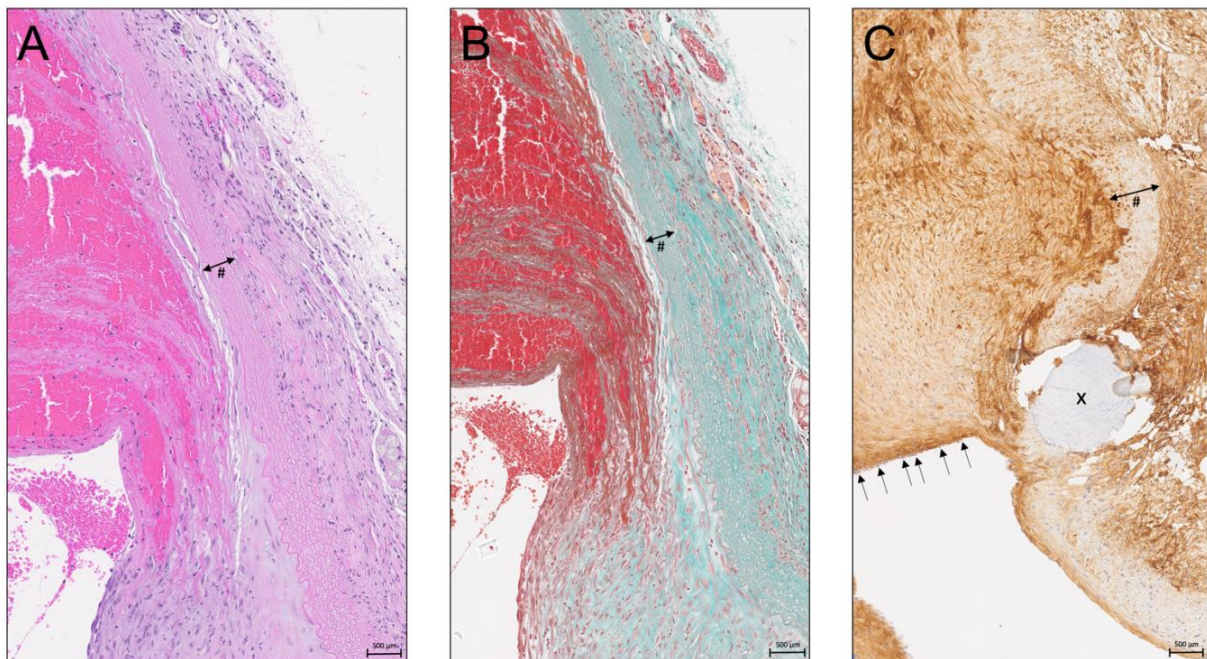


Supplementary Figure 5. Microphotograph of a cross-section shows a vital aneurysm (*) and its parent artery complex without ASA treatment. Proximal left (a), distal left (b), and right CCA (c) are marked.



Supplementary Figure 6. Representative microphotographs depicting thrombus formation.

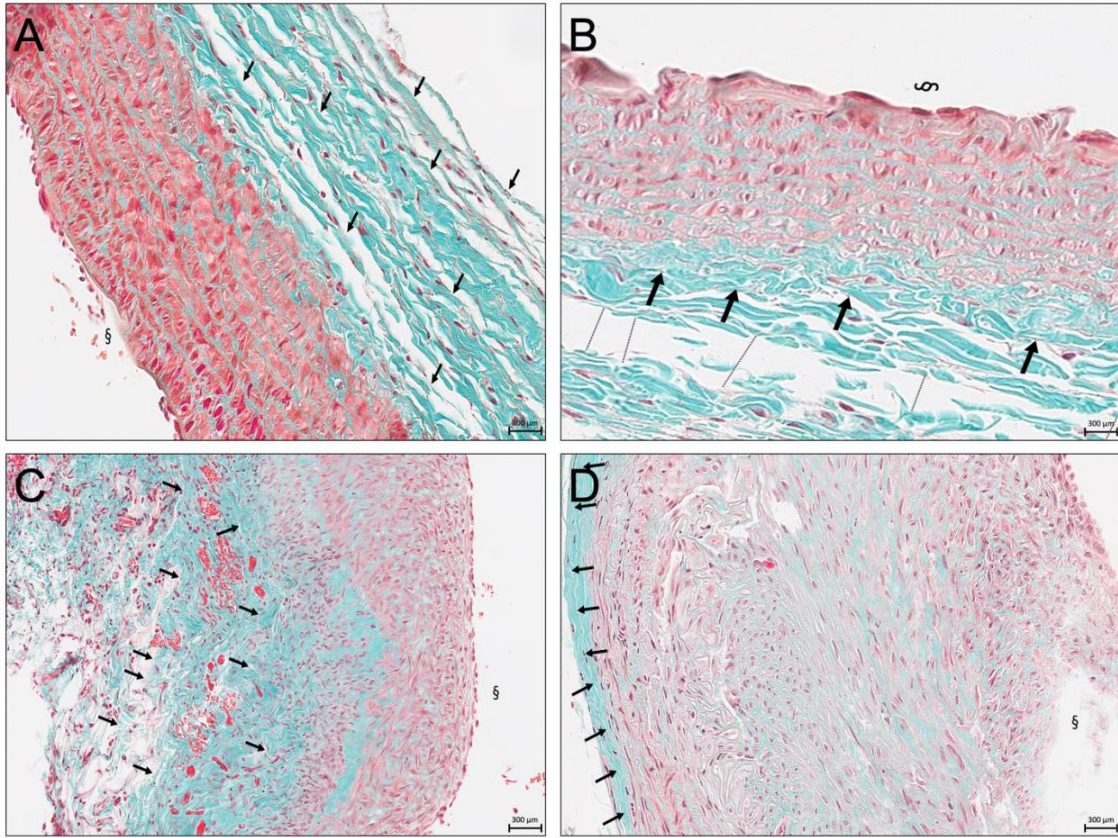
Note the apical thrombus formation with consecutive neointima formation and endothelial lining from the lumen of a decellularized aneurysm without ASA treatment. Staining with HE (A), MASA (B) and F8 (C) are shown. Cell-depleted muscular media (#). (C) endothelial cells demonstrating neointima formation (black arrows). Crosscut (x) of the underlying 9-0 non-absorbable suture material.



Supplementary Figure 7. Representative microphotographs depicting periadventitial fibrosis.

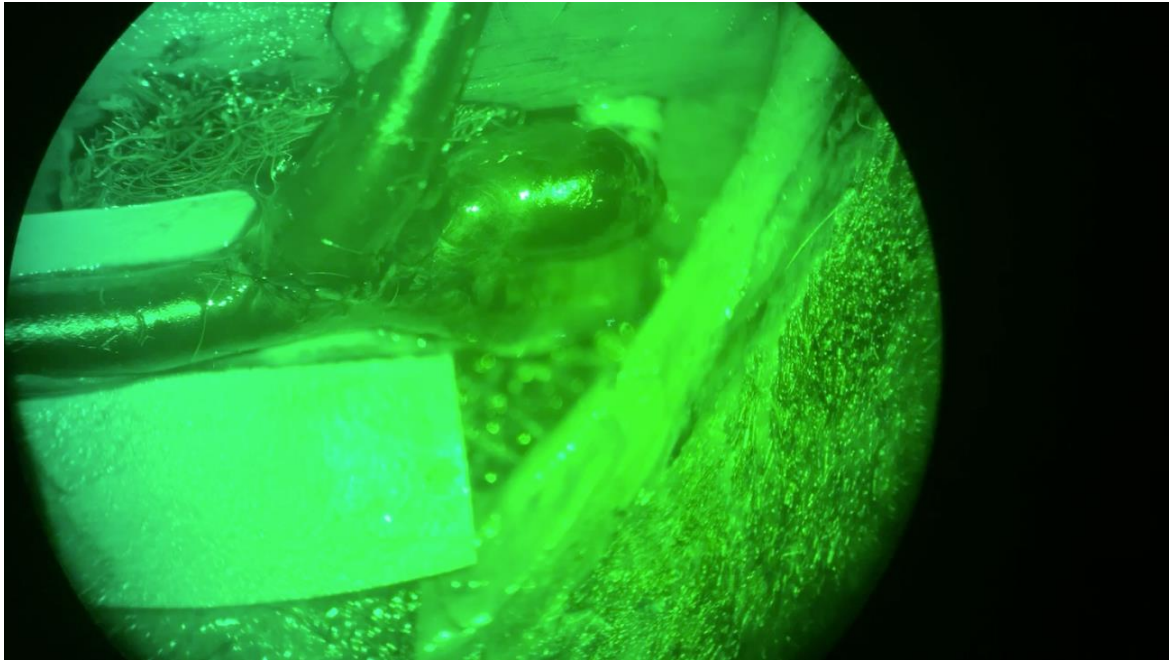
Different magnifications of MASA stained histological samples of vital and elastase-degraded aneurysms treated without and with ASA. Collagen fibers (green) and blood (red). Scale bar: 300 μm .

- (A) Adventitia in a vital aneurysm without ASA treatment. Note the intense periadventitial fibrosis (black arrows).
- (B) Masson-Goldner trichrome staining of the adventitia in vital aneurysm with ASA pretreatment (§ shows the luminal side, black arrows the periadventitial fibrosis). Note the rarefication of collagen fibers (dotted line) compared to (A). Scale bar: 300 μm .
- (C) Masson-Goldner trichrome staining of the adventitia in an elastase treated aneurysm without ASA (§ shows the luminal side of the aneurysm). Note the intensive fibrosis (black arrows), likewise the diffuse infiltration of neutrophils in between (black arrowheads). Scale bar: 300 μm .
- (D) Masson-Goldner trichrome staining of the adventitia in an elastase treated aneurysm with ASA. (D) shows a 40-fold magnification of the outer periadventitia. Note the diminished periadventitial fibrosis (black arrows) compared to (C). Furthermore, no neutrophils can be detected. Scale bar: 300 μm .



Supplementary Videos

Supplementary Video 1. Fluorescence angiography. Video shows an elastase- degraded arterial pouch with consecutive fluorescein application to confirm intraoperative patency.



Supplementary Table 1. Surgery times averaged 164.0 ± 25.0 min (range 122-187) with 51.2 ± 8.6 min (range 42-66) needed for aneurysm creation in the vital group w/o ASA and 170.0 ± 25.0 min (range 148-203) with 48.8 ± 6.4 min (range 42-60) for the w ASA group. Duration of the surgical procedure in the decellularized group w/o ASA was 203.3 ± 43.5 min (range 159-285), for aneurysm creation 72.7 ± 25.0 min (range 50-120); for the w ASA group 148.5 min ± 14.3 min (range 135-172) and 46.3 min ± 9.1 min (range 30-57) were needed. For the elastase w/o ASA group, values were 200.8 min ± 31.9 min (range 158-250 minutes) for surgery in whole, for aneurysm creation 57.5 min ± 13.3 min (range 43-76); the w ASA group values were 186.2 min ± 28.7 min (range 158-240), for aneurysm creation 55.3 min ± 24.7 min (range 26-100).

(A). Surgical characteristics and morphometric measurements of vital aneurysms without medical treatment. Values are expressed as

means \pm SD. * $p_{Vol(BL-FU)} < 0.05$.

<i>n</i>	<i>Weight (g)</i>	<i>Ischemia (min)</i>	<i>Suture time (min)</i>	<i>Stitches (#)</i>	<i>Re-stitches (#)</i>	<i>Surgery (min)</i>	<i>Volume baseline (mm³)</i>	<i>MRT (days)</i>	<i>Volume follow-up (mm³)</i>	<i>CCA left proximal (mm)</i>	<i>CCA left distal (mm)</i>	<i>CCA right (mm)</i>
1	4100.00	98.00	54.00	24	0	187.00	1.96	24	5.00	2.50	2.80	1.80
2	4200.00	121.00	53.00	24	1	183.00	2.35	23	7.73	3.30	2.90	2.50
3	3800.00	102.00	66.00	26	0	163.00	4.71	37	28.03	3.40	3.00	2.60
4	3600.00	67.00	42.00	22	0	122.00	6.28	37	47.37	2.80	2.80	3.20
5	3700.00	88.00	45.00	24	3	180.00	10.99	22	15.82	3.20	3.00	2.80
6	3700.00	89.00	47.00	21	0	149.00	12.56	31	15.11	2.30	2.20	1.90
Mean	3850.00	94.17	51.17	23.50	0.67	164.00	6.48	29.00	19.85	2.92	2.78	2.47
\pm	\pm	\pm	\pm	\pm	\pm	\pm	\pm	\pm	\pm	\pm	\pm	\pm
SD	242.90	17.88	8.61	1.76	1.21	25.04	4.43	6.96	15.69*	0.45	0.30	0.54

Abbreviations: CCA (common carotid artery); CE-3D-MRA (contrast enhanced 3D magnetic resonance angiography); g (gram); min (minute/s); mm³ (cubic millimeter)

(B). Surgical characteristics and morphometric measurement of vital aneurysms with ASA treatment. Values are expressed as means \pm SD.

<i>n</i>	<i>Weight (g)</i>	<i>Ischemia (min)</i>	<i>Suture time (min)</i>	<i>Stitches (#)</i>	<i>Re-stitches (#)</i>	<i>Surgery (min)</i>	<i>Volume baseline (mm³)</i>	<i>MRT (days)</i>	<i>Volume follow-up (mm³)</i>	<i>CCA left proximal (mm)</i>	<i>CCA left distal (mm)</i>	<i>CCA right (mm)</i>
1	3900.00	89.00	44.00	25	0	148.00	12.56	26	14.13	2.70	2.40	2.40
2	3855.00	98.00	51.00	21	0	198.00	9.42	23	10.72	2.50	2.80	2.30
3	3700.00	87.00	47.00	27	0	148.00	11.77	23	17.00	3.30	2.70	2.60
4	3850.00	121.00	60.00	22	0	203.00	7.06	24	23.17	2.60	2.60	2.70
5	3850.00	88.00	49.00	22	1	170.00	8.24	26	14.36	2.90	2.80	2.30
6	3980.00	85.00	42.00	25	0	153.00	10.99	26	4.04	2.50	2.40	2.20
Mean	3855.00	94.67	48.83	23.67	0.17	170.00	10.01	24.67	13.91	2.75	2.62	2.42
\pm	\pm	\pm	\pm	\pm	\pm	\pm	\pm	\pm	\pm	\pm	\pm	\pm
SD	91.35	13.66	6.37	2.34	0.41	25.02	2.13	1.51	6.38	0.31	0.18	0.19

(C). Surgical characteristics and morphometric measurement of decellularized aneurysms without medical treatment. Values are expressed as means \pm SD.

<i>n</i>	<i>Weight (g)</i>	<i>Ischemia (min)</i>	<i>Suture time (min)</i>	<i>Stitches (#)</i>	<i>Re-stitches (#)</i>	<i>Surgery (min)</i>	<i>Volume baseline (mm³)</i>	<i>MRT (days)</i>	<i>Volume follow-up (mm³)</i>	<i>CCA left proximal (mm)</i>	<i>CCA left distal (mm)</i>	<i>CCA right (mm)</i>
1	3400.00	159.00	120.00	22	0	285.00	8.83	83	14.44	3.10	2.50	2.30
2	3900.00	177.00	76.00	19	0	208.00	4.71	33	4.00	2.70	2.40	2.30
3	4200.00	121.00	68.00	22	0	198.00	20.60	29	14.34	2.70	2.70	2.70
4	3300.00	107.00	50.00	23	3	192.00	6.28	40	19.62	3.10	3.30	2.80
5	3400.00	109.00	55.00	29	0	159.00	11.77	40	19.62	3.40	2.90	2.70
6	3700.00	104.00	67.00	20	0	178.00	7.06	41	14.56	-	-	-
Mean	3650.00	129.50	72.67	22.50	0.50	203.33	9.88	44.33	14.43	3.00	2.76	2.56
\pm	\pm	\pm	\pm	\pm	\pm	\pm	\pm	\pm	\pm	\pm	\pm	\pm
SD	350.71	30.91	25.03	3.51	1.23	43.49	5.79	19.53	9.02	0.30	0.36	0.24

(D). Surgical characteristics and morphometric measurements of decellularized aneurysms with ASA treatment. Values are expressed as

means \pm SD.

<i>n</i>	<i>Weight (g)</i>	<i>Ischemia (min)</i>	<i>Suture time (min)</i>	<i>Stitches (#)</i>	<i>Re-stitches (#)</i>	<i>Surgery (min)</i>	<i>Volume baseline (mm³)</i>	<i>MRT (days)</i>	<i>Volume follow-up (mm³)</i>	<i>CCA left proximal (mm)</i>	<i>CCA left distal (mm)</i>	<i>CCA right (mm)</i>
1	3760.00	100.00	57.00	24	0	160.00	12.56	26	18.84	2.50	1.90	2.10
2	3800.00	77.00	49.00	24	0	143.00	15.70	25	11.77	2.60	2.60	2.80
3	3760.00	87.00	50.00	25	0	140.00	15.70	24	17.66	2.80	2.50	2.00
4	3550.00	89.00	48.00	20	2	172.00	15.70	26	10.99	3.00	2.80	2.60
5	3700.00	88.00	44.00	23	0	141.00	9.42	24	14.13	2.80	2.90	2.60
6	3800.00	66.00	30.00	23	0	135.00	12.56	31	34.34	3.20	3.30	2.50
Mean	3728.33	84.50	46.33	23.17	0,33	148.50	13.61	26.00	17.95	2.82	2.67	2.43
\pm	\pm	\pm	\pm	\pm	\pm	\pm	\pm	\pm	\pm	\pm	\pm	\pm
SD	94.75	11.64	9.05	1.72	0,82	14.32	2.56	2.61	8.61	0.26	0.47	0.31

(E). Surgical characteristics and morphometric measurements of elastase aneurysms without medical treatment. Values are expressed as

means \pm SD. * $p_{Vol(BL-FU)} < 0.05$.

<i>n</i>	<i>Weight (g)</i>	<i>Ischemia (min)</i>	<i>Suture time (min)</i>	<i>Stitches (#)</i>	<i>Re-stitches (#)</i>	<i>Surgery (min)</i>	<i>Volume baseline (mm³)</i>	<i>MRT (days)</i>	<i>Volume follow-up (mm³)</i>	<i>CCA left proximal (mm)</i>	<i>CCA left distal (mm)</i>	<i>CCA right (mm)</i>
1	3400.00	114.00	76.00	26	0	158.00	9.42	29	12.26	2.90	2.60	2.70
2	3400.00	135.00	43.00	27	0	180.00	10.99	32	46.16	3.50	2.80	2.50
3	3900.00	197.00	70.00	27	0	250.00	6.59	31	10.10	3.50	3.20	3.30
4	4200.00	140.00	45.00	28	0	208.00	9.42	30	24.00	3.00	2.60	2.10
5	3660.00	109.00	53.00	18	0	192.00	8.24	25	8.00	2.80	2.80	2.80
6	3200.00	115.00	58.00	24	1	217.00	3.53	46	25.16	2.70	2.80	3.10
Mean	3626.67	135.00	57.50	25.00	0.17	200.83	8.03	32.17	20.95	3.07	2.80	2.75
\pm	\pm	\pm	\pm	\pm	\pm	\pm	\pm	\pm	\pm	\pm	\pm	\pm
SD	371.30	32.82	13.31	3.69	0.41	31.87	2.64	7.20	14.31*	0.35	0.22	0.43

(F). Surgical characteristics and morphometric measurements of elastase aneurysms with ASA treatment. Values are expressed as means

± SD. * p_{Vol(BL-FU)} < 0.05.

<i>n</i>	<i>Weight (g)</i>	<i>Ischemia (min)</i>	<i>Suture time (min)</i>	<i>Stitches (#)</i>	<i>Re-stitches (#)</i>	<i>Surgery (min)</i>	<i>Volume baseline (mm³)</i>	<i>MRT (days)</i>	<i>Volume follow-up (mm³)</i>	<i>CCA left proximal (mm)</i>	<i>CCA left distal (mm)</i>	<i>CCA right (mm)</i>
1	3700.00	158.00	100.00	24	0	240.00	18.84	27	26.70	3.30	3.20	2.00
2	4200.00	81.00	26.00	22	2	168.00	7.06	23	32.36	3.00	2.70	2.50
3	3600.00	99.00	45.00	20	0	182.00	7.06	33	13.84	2.90	2.80	2.40
4	3750.00	114.00	58.00	23	1	179.00	9.42	45	11.65	3.30	3.40	3.00
5	3300.00	109.00	57.00	21	0	190.00	8.24	44	10.17	2.10	2.00	2.00
6	3700.00	80.00	46.00	21	0	158.00	8.38	40	21.98	-	-	-
Mean	3625.00	106.83	55.33	21.83	0.50	186.17	9.91	35.33	19.45	2.92	2.82	2.32
±	±	±	±	±	±	±	±	±	±	±	±	±
SD	357.42	28.72	24.74	1.47	0.84	28.65	4.48	9.14	8.99*	0.49	0.54	0.50